



In situ AFM and Raman spectroscopy study of the crystallization behavior of Ge₂Sb₂Te₅ films at different temperature

Yongkuan Wu, Kun Liu, Dawei Li, Yingnan Guo, Shi Pan*

School of Physics and Optoelectronic Technology, Dalian University of Technology, Dalian 116023, China

ARTICLE INFO

Article history:

Received 8 September 2011

Received in revised form

26 September 2011

Accepted 5 October 2011

Available online 12 October 2011

Keywords:

Ge₂Sb₂Te₅

Crystallization

AFM

Raman spectroscopy

Temperature control

ABSTRACT

Using in situ atomic force microscope (AFM) and Raman spectroscopy, the real-time crystallization properties of Ge₂Sb₂Te₅ films at different temperature were characterized. The given AFM topograph and phase images revealed that the structure of amorphous Ge₂Sb₂Te₅ films began to change at a temperature of as low as 100 °C. When the temperature reached 130 °C, some crystal fragments had formed at the film surface. Heating up to 160 °C, the size of the visible crystal fragments increased, but decreased at a higher temperature of 200 °C. When the Ge₂Sb₂Te₅ film was cooled down to room temperature (RT) from 200 °C, the crystal fragments divided into crystal grains due to the absence of heating energy. The Raman spectra at different temperature further verified the structure evolution of the Ge₂Sb₂Te₅ film with temperature. This work is of significance for the preparation of Ge₂Sb₂Te₅ films and the erasing of data.

© 2011 Elsevier B.V. All rights reserved.

1. Introduction

Ge₂Sb₂Te₅ ternary alloy is used as rewritable recording media owing to its outstanding phase change characteristics [1,2]. The distinct contrast of Ge₂Sb₂Te₅ films in resistivity and reflectivity between crystalline and amorphous phases is fit for information storage. The data can be recorded by writing amorphous dots on a crystalline background with a short high-power pulse, and can be erased through a continuous mild annealing.

The understanding of the crystallization process is of great importance for the preparation of Ge₂Sb₂Te₅ films and the erasing of data. The structure and morphology differences between crystalline and amorphous phases of Ge₂Sb₂Te₅ films have been extensively studied using X-ray diffraction (XRD), transmission electron microscopy (TEM), Raman spectroscopy, and atomic force microscope (AFM) [1,3–12]. Most of them detected the structure and morphology of crystalline Ge₂Sb₂Te₅ films at room temperature (RT). Through in situ TEM characterization, the nucleation and grain growth of amorphous Ge₂Sb₂Te₅ films at elevated temperature has been observed closely which provides valuable information concerning the crystallization process [13–17]. However, for TEM study, the samples have to be thin enough, which makes the sample preparation complicated, and the electron beam used for imaging would affect the crystallization process [16–18].

For example, in Kooi and co-worker's work, the influence of electron beam exposure on crystallization of Sb_xTe films was studied, and found that the crystal growth velocity was strongly increased under an electron beam exposure [17].

The aim of this work is to examine the real-time crystallization behavior of amorphous Ge₂Sb₂Te₅ films, and focuses on the morphology and structure variation at different temperature. AFM, compared with TEM, can acquire nanoscale three-dimension morphology information of Ge₂Sb₂Te₅ films without heating effect and complicated sample preparation. While Raman spectroscopy, a powerful structure detector for its high information content and simple sample preparation [19] is suitable for probing the crystallinity of Ge₂Sb₂Te₅ films. Therefore, AFM and Raman spectroscopy were combined together to monitor the morphology and structure evolution of amorphous Ge₂Sb₂Te₅ films at different temperature.

2. Experiments

Amorphous Ge₂Sb₂Te₅ films (Ge₂Sb₂Te₅(50 nm)/Al(200 nm)/BK7glass) were prepared by radio frequency magnetron sputtering at RT using a stoichiometric target. During AFM and Raman experiments, as-prepared Ge₂Sb₂Te₅ films were placed on a temperature-control sample stage, and were protected with nitrogen in a sealed sample chamber. The temperature of the samples was controlled through a Lakeshore temperature controller (precision: ±0.1 °C) with a heating rate of 5 °C/min and kept constant for 10 min before AFM and Raman survey.

* Corresponding author. Tel.: +86 411 84707863; fax: +86 411 84709304.
E-mail address: span@dlut.edu.cn (S. Pan).

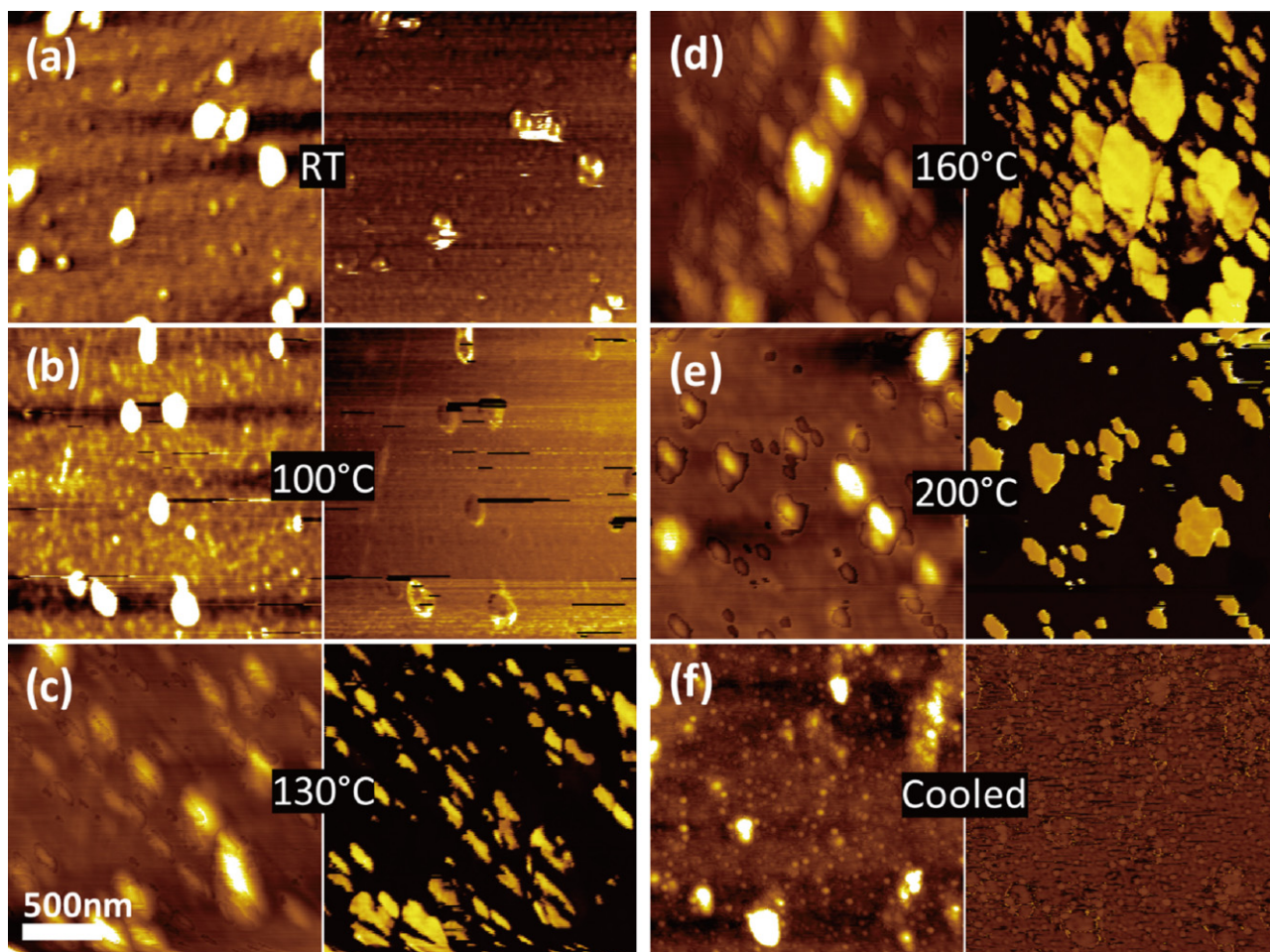


Fig. 1. In situ AFM topograph (left) and phase (right) images of the as-prepared $\text{Ge}_2\text{Sb}_2\text{Te}_5$ film at different temperature, (a) RT, (b) 100°C , (c) 130°C , (d) 160°C , (e) 200°C , (f) cooled to RT. The height-scale of topograph and phase images from (a) to (f) is (5.6 nm, 12.7°), (3.8 nm, 4.0°), (22.3 nm, 169.7°), (30.9 nm, 155.4°), (14.4 nm, 263.7°), (17.6 nm, 217.6°), respectively.

The topograph and phase images of the $\text{Ge}_2\text{Sb}_2\text{Te}_5$ films at different temperature were obtained with tapping-mode AFM (Agilent PicoPlus) in situ. The crystallinity of the $\text{Ge}_2\text{Sb}_2\text{Te}_5$ film was detected using XRD (Bruker, D8-Discover). Raman scattering was dispersed by a Renishaw inVia Raman spectrometer, and back scattering light was collected with an air-cooled CCD array detector. The spectra were recorded with an accumulation time of 100 s. Laser intensity (632.8 nm HeNe laser) was kept below $10\ \mu\text{W}$ and laser beam was defocused (about $20\ \mu\text{m}$ in diameter) to reduce unwanted heating effect.

3. Results and discussion

The morphology evolution of the as-prepared $\text{Ge}_2\text{Sb}_2\text{Te}_5$ film at different temperature is displayed in Fig. 1. It is observed in Fig. 1(a) that the $\text{Ge}_2\text{Sb}_2\text{Te}_5$ film at RT exhibits an unordered surface structure and a uniform phase, which indicates that the as-prepared $\text{Ge}_2\text{Sb}_2\text{Te}_5$ film is typically amorphous. The small fluctuations in the phase image were caused by the undulations of the film surface. XRD pattern of the as-prepared $\text{Ge}_2\text{Sb}_2\text{Te}_5$ film (black line in Fig. 2, with only a small mountain centered at $2\theta \approx 29^\circ$) further confirms that its structure is amorphous. When the temperature was increased to 100°C , many small grains emerged in the topograph image of the $\text{Ge}_2\text{Sb}_2\text{Te}_5$ film (Fig. 1(b)), though the phase image was still uniform. Increasing the temperature to 130°C , many small mounts and “defects” emerged in the topograph image, and a lot of bright specks appeared in the phase image (Fig. 1(c)). The whole

phase image at 130°C was taken up with two different parts (dark region and bright specks), and the bright specks were corresponding to the defects in the topograph image rather than the small mounts (see Fig. 3).

Based on AFM imaging theory, different phase regions reveal different mechanical property of sample surface [20]. Thus, the two

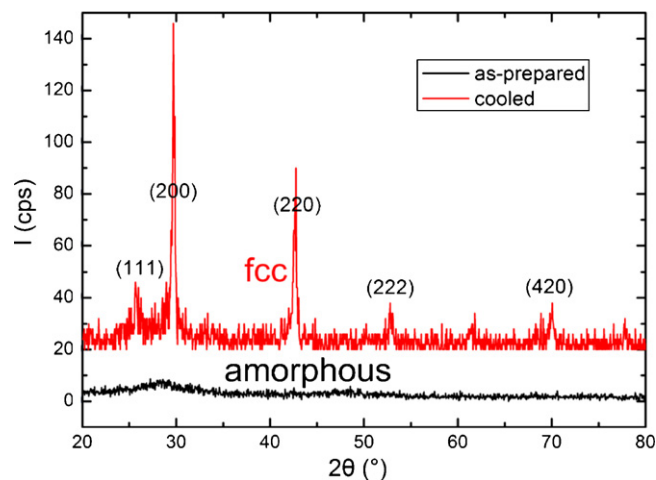


Fig. 2. XRD patterns of as-prepared (lower) and treated (upper, cooled to RT from 200°C) $\text{Ge}_2\text{Sb}_2\text{Te}_5$ films.

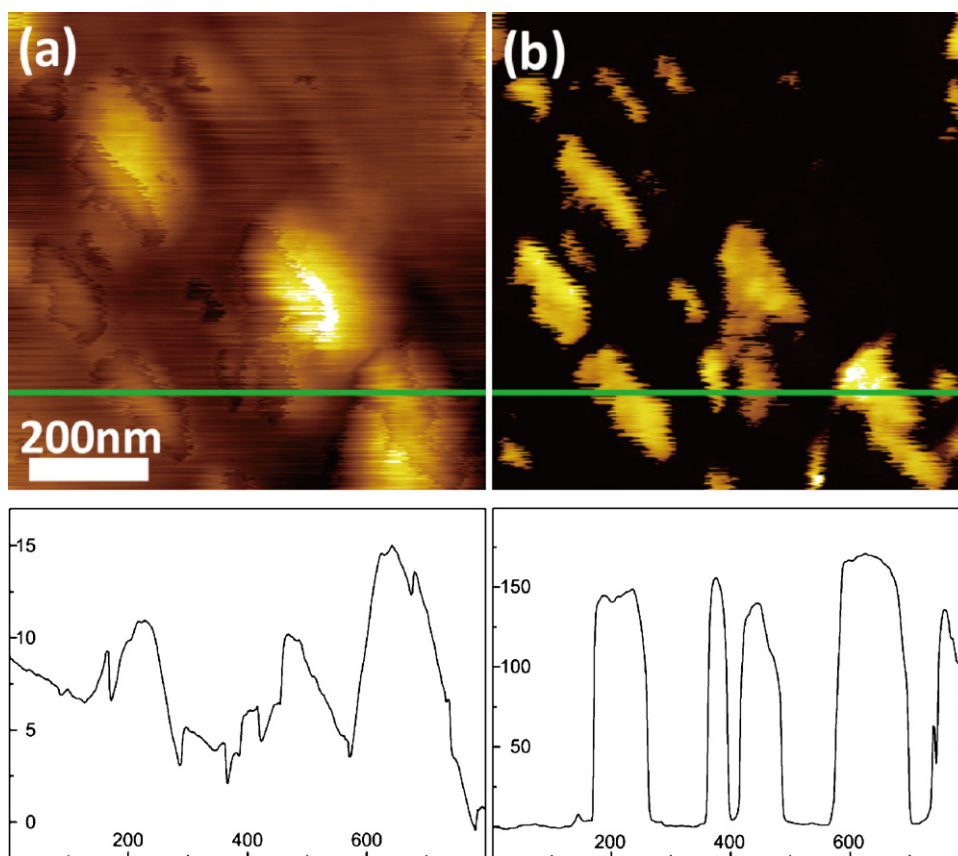


Fig. 3. Enlarged topograph (a) and phase (b) images of the $\text{Ge}_2\text{Sb}_2\text{Te}_5$ film at 130°C ; the curves at the bottom are corresponding cross-section views of the green lines, and the height-scale of the topograph and phase images is (17.2 nm, 170.3°).

phase distribution in Fig. 1(c) manifests that the $\text{Ge}_2\text{Sb}_2\text{Te}_5$ film at 130°C were consisted with two different components. It has been reported that the density of face centered cubic (fcc) $\text{Ge}_2\text{Sb}_2\text{Te}_5$ crystal is $\sim 6.8\%$ bigger than that of the amorphous phase, and this resulted in the slight sinking of the $\text{Ge}_2\text{Sb}_2\text{Te}_5$ crystal compared to the amorphous background [1]. Thus, it can be inferred from the AFM images that the bright specks (defects) were fcc crystals and the dark region was amorphous background.

With further increasing the temperature (160°C), the small mounts and the bright specks (defects) got larger (Fig. 1(d)). However, when the temperature reached 200°C , the small mounts and the bright specks shrank (Fig. 1(e)). Fig. 1(f) shows the AFM images of the $\text{Ge}_2\text{Sb}_2\text{Te}_5$ film cooled to RT from 200°C . It is observed that the bright specks disappeared, the two-phase distribution got obscure, and many spherical grains emerged in the topograph image. It is noticed that the height-scale of the phase image was still as large as that at high temperatures ($130\text{--}200^\circ\text{C}$), indicating that the surface of the $\text{Ge}_2\text{Sb}_2\text{Te}_5$ film was still consisted of two phases (amorphous and crystalline). While XRD pattern of the $\text{Ge}_2\text{Sb}_2\text{Te}_5$ film cooled to RT from 200°C is shown in Fig. 2, and five obvious diffraction peaks verified that the major component of the film was fcc crystal.

According to the AFM images and the known crystallization properties of $\text{Ge}_2\text{Sb}_2\text{Te}_5$ films [2,3,5,13,14,18], the crystallization process of the $\text{Ge}_2\text{Sb}_2\text{Te}_5$ film is described as follows. At RT, the as-prepared $\text{Ge}_2\text{Sb}_2\text{Te}_5$ film is amorphous (Fig. 4(a)) with unordered structure. When the temperature reached 100°C , some small spherical crystal nuclei formed (small grains in the topograph image of Fig. 1(b)), but could not grow into big crystal grains for insufficient energy supply, while the structure of the $\text{Ge}_2\text{Sb}_2\text{Te}_5$ film was sort of ordered and prepared for crystallization (Fig. 4(b)).

According to previous works, amorphous $\text{Ge}_2\text{Sb}_2\text{Te}_5$ films began to crystallize in the range of $140\text{--}180^\circ\text{C}$ upon annealing, and the structure of $\text{Ge}_2\text{Sb}_2\text{Te}_5$ films in the phase transition region is a mixture of three components (amorphous, crystal nucleus and crystalline) [5,14]. In our research, some spherical crystal nuclei had already grown into big crystal fragments at the film surface at 130°C (Fig. 4(c)), and this process also caused the appearance of those small mounts (Fig. 1(c)). As the temperature got higher (160°C), the crystal fragments grew into bigger ones, and most of the film surface was covered with crystalline phase (Fig. 4(d)). However, heating up to 200°C , the visible crystal fragments at the film surface got smaller (Fig. 1(e)). According to previous TEM works, the uncapped $\text{Ge}_2\text{Sb}_2\text{Te}_5$ films initially crystallized at the film surface, and further proceeded by the growth of the crystals through the thickness of the films [13,18]. Since AFM just detects the surface of the sample, the sinking of crystal fragments due to its higher density than amorphous phase may cause that the visible crystal fragments got smaller, even though the crystal fragments got larger beneath the surface. When the $\text{Ge}_2\text{Sb}_2\text{Te}_5$ film was cooled to RT from 200°C , the crystal fragments divided into many big crystal grains due to the absence of heating energy (Fig. 4(f)).

Above results revealed that the morphology and crystallinity of the $\text{Ge}_2\text{Sb}_2\text{Te}_5$ film varied at different temperature. Therefore, the choice of annealing temperature is crucial to obtain superior crystalline $\text{Ge}_2\text{Sb}_2\text{Te}_5$ films with smooth and well-crystallized surface. Besides, the annealing time should be another important factor for the preparation of crystalline $\text{Ge}_2\text{Sb}_2\text{Te}_5$ films. But, the influence of annealing time on the crystallinity of the $\text{Ge}_2\text{Sb}_2\text{Te}_5$ film was not discussed here for the following two reasons. (1), the increase of the temperature inevitably caused the deformation of the sample and the decrease of the tip-sample distance duo to heat expansion,

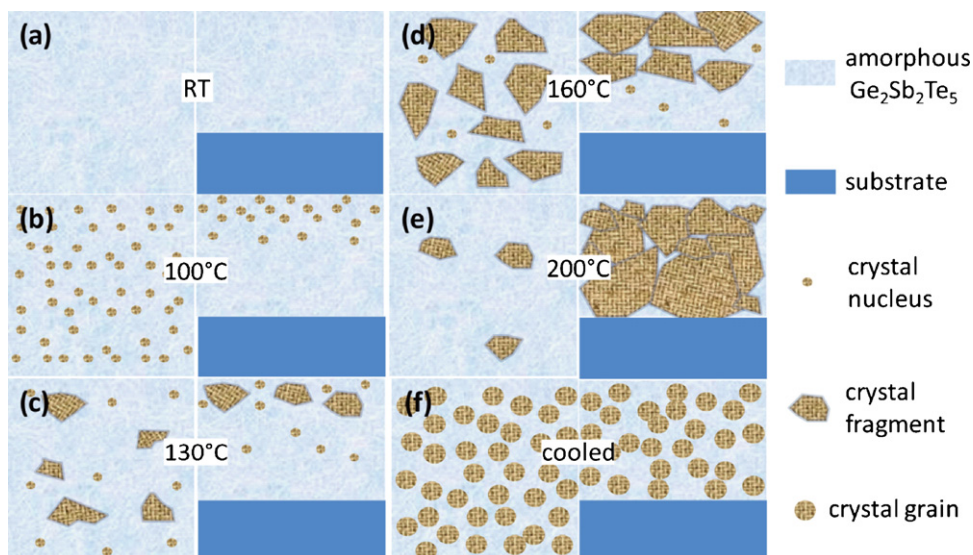


Fig. 4. Sketch of the crystallization process of the $\text{Ge}_2\text{Sb}_2\text{Te}_5$ film at different temperature, (a) RT, (b) 100°C , (c) 130°C , (d) 160°C , (e) 200°C , (f) cooled to RT. The lefts of these images are top views, and the rights are cross-section views.

to avoid damaging the AFM tip, we withdrew the tip before the temperature-rise. (2), the increase of the temperature also caused the downshift of the resonance frequency of the AFM tip, the scanning frequency of AFM tip must be reselected at a new temperature. Thereby, it took at least 10 min to enter the scanning status for a new temperature, and this resulted in that the initial crystallization process of the $\text{Ge}_2\text{Sb}_2\text{Te}_5$ film at different temperature was missed. Although the succeeding information was available, the given AFM images (not shown here) revealed that the structure of the $\text{Ge}_2\text{Sb}_2\text{Te}_5$ film had got stable from then on. In a word, the dynamic information concerning the initial crystallization process of the $\text{Ge}_2\text{Sb}_2\text{Te}_5$ film was not obtained.

Fig. 5 shows the corresponding Raman spectra of the as-prepared $\text{Ge}_2\text{Sb}_2\text{Te}_5$ film at different temperature. At RT, no any Raman peak was observed in our experiments which is different from the previous results (a broad peak around 150 cm^{-1} which was attributed to the amorphous Te–Te stretching) [4,10]. As the temperature reached 100°C , a broad rectangular peak between 160

and 190 cm^{-1} was observed, and this is considered as an implication of the nucleation or the slight crystallization of the $\text{Ge}_2\text{Sb}_2\text{Te}_5$ film. The intensity of the broad rectangular peak increased at higher temperature (130°C , 160°C), which implied the $\text{Ge}_2\text{Sb}_2\text{Te}_5$ film was further crystallized. At 200°C , the broad peak got stronger tempestuously and divided into three small peaks (red triangles), and another broad peak around 330 cm^{-1} appeared. Moreover, several new peaks were observed (black stars), which suggested that the $\text{Ge}_2\text{Sb}_2\text{Te}_5$ film was well crystallized. The Raman characteristics of the $\text{Ge}_2\text{Sb}_2\text{Te}_5$ film at 200°C present evidence for the above speculation that the crystal fragments got larger beneath the surface though the visible crystal fragments at the film surface got smaller (Fig. 1(e)). When the $\text{Ge}_2\text{Sb}_2\text{Te}_5$ film was cooled to RT from 200°C , the peak intensity decreased, but was still stronger than that at 130°C which manifests that the crystallinity of the $\text{Ge}_2\text{Sb}_2\text{Te}_5$ film cooled to RT from 200°C is better than that at 130°C . The above analysis of Raman data just reveals a small part of the information concerning the crystallization process of the $\text{Ge}_2\text{Sb}_2\text{Te}_5$ film, while the identification and quantitative analysis of the Raman spectroscopy are of great importance and are in progress.

4. Conclusion

The real-time crystallization behavior of $\text{Ge}_2\text{Sb}_2\text{Te}_5$ films at different temperature has been investigated by combining AFM with Raman spectroscopy. This research presented that the structure and morphology of the $\text{Ge}_2\text{Sb}_2\text{Te}_5$ film cooled to RT was different with that at high temperature. At $130\text{--}200^\circ\text{C}$, there were many crystal fragments exposed at the film surface, and the two-phase distribution is clear. As the $\text{Ge}_2\text{Sb}_2\text{Te}_5$ film was cooled to RT from 200°C , the crystal fragments divided into crystal grains, and the two-phase distribution became obscure. Moreover, owing to the crystallinity variation of the $\text{Ge}_2\text{Sb}_2\text{Te}_5$ film with temperature, the choice of annealing temperature is crucial to obtain superior crystalline $\text{Ge}_2\text{Sb}_2\text{Te}_5$ films. To further understand the crystallization process of the $\text{Ge}_2\text{Sb}_2\text{Te}_5$ films, high-speed AFM imaging during the initial crystallization process is necessary, and the identification and quantitative analysis of the Raman spectroscopy are of great importance.

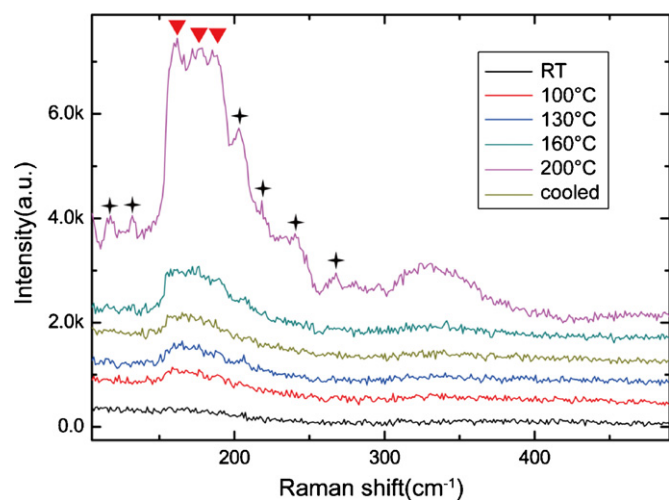


Fig. 5. Raman spectra of the as-prepared $\text{Ge}_2\text{Sb}_2\text{Te}_5$ film at different temperature, from the bottom: RT, 100°C , 130°C , cooled to RT, 160°C , 200°C , and the laser intensity (632.8 nm HeNe laser) was kept below $10\text{ }\mu\text{W}$ and laser beam was defocused (about $20\text{ }\mu\text{m}$ in diameter) to reduce unwanted heating effect.

Acknowledgements

This work was supported by The National Natural Sciences Foundation of China (10974025). Thanks Prof. Qingyu Zhang and Jinsong Wei for the help and valuable discussion.

References

- [1] M. Wuttig, R. Detemple, I. Friedrich, W. Njoroge, I. Thomas, V. Weidenhof, H.W., W. Irgens, S. Ziegler, The quest for fast phase change materials, *Journal of Magnetism and Magnetic Materials* 249 (2002) 492–498.
- [2] X. Miao, L. Shi, H. Lee, J. Li, R. Zhao, P. Tan, K. Lim, H. Yang, T. Chong, Temperature dependence of phase-change random access memory cell, *Japanese Journal of Applied Physics Part 1 Regular Papers Short Notes and Review Papers* 45 (2006) 3955.
- [3] V. Weidenhof, I. Friedrich, S. Ziegler, M. Wuttig, Atomic force microscopy study of laser induced phase transitions in GeSbTe, *Journal of Applied Physics* 86 (1999) 5879.
- [4] J. Tominaga, N. Atoda, Study of the crystallization of GeSbTe films by Raman spectroscopy, *Japanese Journal of Applied Physics* 38 (1999) L322–L323.
- [5] E. Morales-Sánchez, E. Prokhorov, Y. Vorobiev, J. González-Hernández, The nature of the crystallization nuclei in Ge₂Sb₂Te₅ alloys, *Solid State Communications* 122 (2002) 185–188.
- [6] Y.J. Park, J.Y. Lee, Y.T. Kim, In situ transmission electron microscopy study of the nucleation and grain growth of Ge₂Sb₂Te₅ thin films, *Applied Surface Science* 252 (2006) 8102–8106.
- [7] H. Yoon, W. Jo, E. Cho, S. Yoon, M. Kim, Microstructure and optical properties of phase-change Ge-Sb-Te nanoparticles grown by pulsed-laser ablation, *Journal of Non-crystalline Solids* 352 (2006) 3757–3761.
- [8] M. Jang, S. Park, D. Lim, M.H. Cho, K. Do, D.H. Ko, H. Sohn, Phase change behavior in oxygen-incorporated Ge₂Sb₂Te₅ films, *Applied Physics Letters* 95 (2009) 012102–012103.
- [9] S. Meister, S.B. Kim, J.J. Cha, H.S.P. Wong, Y. Cui, In situ transmission electron microscopy observation of nanostructural changes in phase-change memory, *ACS Nano* (2011).
- [10] L. Bo, S. Zhi-Tang, Z. Ting, F. Song-Lin, C. Bomy, Raman spectra and XPS studies of phase changes in Ge₂Sb₂Te₅ films, *Chinese Physics* 13 (2004) 1947.
- [11] N. Kato, I. Konomi, Y. Seno, T. Motohiro, In situ X-ray diffraction study of crystallization process of GeSbTe thin films during heat treatment, *Applied Surface Science* 244 (2005) 281–284.
- [12] R. Pandian, B.J. Kooi, G. Palasantzas, J. De Hosson, A. Pauza, Nanoscale electrolytic switching in phase-change chalcogenide films, *Advanced Materials* 19 (2007) 4431–4437.
- [13] T.H. Jeong, M.R. Kim, H. Seo, S.J. Kim, S.Y. Kim, Crystallization behavior of sputter-deposited amorphous Ge₂Sb₂Te₅ thin films, *Journal of Applied Physics* 86 (1999) 774–778.
- [14] G. Ruitenberg, A. Petford-Long, R. Doole, Determination of the isothermal nucleation and growth parameters for the crystallization of thin Ge₂Sb₂Te₅ films, *Journal of Applied Physics* 92 (2002) 3116–3123.
- [15] S.A. Song, W. Zhang, H. Sik Jeong, J.G. Kim, Y.J. Kim, In situ dynamic HR-TEM and EELS study on phase transitions of Ge₂Sb₂Te₅ chalcogenides, *Ultramicroscopy* 108 (2008) 1408–1419.
- [16] E. Rimini, R. De Bastiani, E. Carria, M. Grimaldi, G. Nicotra, C. Bongiorno, C. Spinella, Crystallization of sputtered-deposited and ion implanted amorphous Ge₂Sb₂Te₅ thin films, *Journal of Applied Physics* 105 (2009) 123502–123506.
- [17] R. Pandian, B.J. Kooi, J.T.M. De Hosson, A. Pauza, Influence of electron beam exposure on crystallization of phase-change materials, *Journal of Applied Physics* 101 (2007) 053529.
- [18] B. Kooi, W. Groot, J.T.M. De Hosson, In situ transmission electron microscopy study of the crystallization of GeSbTe, *Journal of Applied Physics* 95 (2004) 924.
- [19] Y. Wu, K. Liu, K. Song, S. Pan, Three powerful research tools from single cells into single molecules: AFM, laser tweezers, and Raman spectroscopy, *Applied Biochemistry and Biotechnology* (2011) 1–12.
- [20] S. Magonov, V. Elings, M.H. Whangbo, Phase imaging and stiffness in tapping-mode atomic force microscopy, *Surface science* 375 (1997) L385–L391.